SEMICONDUCTOR PHYSICS

THGG15 Microcrystal size and shape effects on the Raman spectrum of solids

I. H. CAMPBELL, P. M. FAUCHET, Princeton U., Department of Electrical Engineering, Princeton, NJ 08544.

We present results of a theoretical calculation of the Raman spectrum in microcrystalline solids.[1] In our model, which is based on the original treatment of Richter *et al.*,[2] the phonons are confined to the microcrystal. When the size decreases below 30 nm typically, the optic phonon Stokes line shifts, broadens, and becomes asymmetric because nonzone-center phonons start contributing to the line. We have explicitly computed the one-phonon Stokes line for small spheres, columns, and slabs in semiconductors such as Si and GaAs. The choice of the confinement function for the phonons was made after a comparison between data for Si spherical micrograins and theoretical results obtained by assuming different confinement functions. The best fit occurred for a Gaussian confinement function with near-zero amplitude at the grain boundary. We thus kept that function for all calculations.

Figure 1 compares our theory to data obtained by us and others[2,3] for silicon spherical micrograins. From the trend in the data and from independent measurements of size performed by x-ray scattering, we confirm that the Gaussian confinement function is most appropriate. Figure 2 compares theory for Gaussian confinement function in spheres, columns, and slabs with data obtained for spherical micrograins and slabs of silicon. The agreement is good, especially in view of the simplicity of the model. No data were available on columns or rods. We will show data obtained on porous silicon, which exhibits a well-defined columnar structure. Our results explain the spectra obtained in Ref. 4 on 4-nm thick Si films prepared by oxidation.

Data obtained on isolated spherical micrograins produced by gas evaporation[5] could not be fitted by our theory. The Raman spectrum was very broad and amorphouslike for sizes as large as 8 nm. In our model, the effects of surface phonons are neglected. This approximation is valid when the interface between the grains and the surrounding matrix is heavily damped. In isolated grains, the amplitude of the surface phonons may remain large.

With the goal of improving our fit, for example, to include the above-mentioned results, we are investigating experimentally the role of surface phonons in microcrystals. We will also present experimental and theoretical results of the two-phonon Stokes spectrum in microcrystals. Higher-order Raman processes show good promise in distinguishing between the effects of crystal size and those of stress or strain. **(Poster paper)**

1. I. H. Campbell and P. M. Fauchet, submitted for publication.
2. H. Richter, Z. P. Wang, and L. Ley, Solid State Commun. **39,** 625 (1981).
3. Z. Iqbal and S. Veprek, J. Phys. C **15,** 377 (1982).
4. D. V. Murphy and S. R. J. Brueck, Mater. Res. Soc. Symp. Proc. **17,** 81 (1983).
5. T. Okada, T. Iwaki, H. Kasahara, and K. Yamamoto, J. Phys. Soc. Jpn. **54,** 1173 (1985).

THGG16 Stimulated Raman gain spectroscopy of gallium arsenide

S. M. BECK, J. E. WESSEL, Aerospace Corporation, Chemistry & Physics Laboratory, P.O. Box 92957, Los Angeles, CA 90009.

Even though Raman scattering of semiconductor materials has been studied intensively for over two decades, new experiments continue to reveal information of fundamental importance concerning mechanisms. Recent studies of gallium arsenide (GaAs)[1] suggest that impurity-induced scattering provides a major contribution to Raman intensity observed near $E_0 + \Delta_0$, the energy range most studied. Impurity-induced scattering should be independent of the phonon wave vector and thus be observable in the forward direction (where q is near zero), whereas intrinsic forbidden scattering should be negligible in the forward direction. Therefore, forward scattering provides a direct test of mechanisms.

We studied forward scattering at photon energies approaching E_0. We report the first observation of strong symmetry selection rules for forward Raman scattering by LO phonons for parallel incident and scattered light polarizations in bulk GaAs. These results are described by intrinsic scattering by the deformation potential mechanism and are consistent with predictions of the q^2-dependent Frohlich mechanism. We extended theoretical impurity scattering calculations previously used[1] to explain scattering in the $E_0 + \Delta_0$ region to below band gap regions and conclude that the previous model predicts that impurity scattering should prevail below band gap. These observations suggest that above band gap scattering models may require modification to include surface effects introduced by the short penetration depths associated with above band gap excitation. **(Poster paper)**

1. J. Menendez and M. Cardona, Phys. Rev. **31,** 3696 (1985).

PHYSICS OF ULTRAPOWERFUL LASER-MATTER INTERACTIONS

THGG17 Measurement of nonlinear optical parameters and recombination times in InSb

HUGH A. MacKENZIE, G. R. ALLAN, J. J. HUNTER, BRIAN S. WHERRETT, Heriot-Watt U., Physics Department, Edinburgh EH14 4AS, U.K.

The nonlinear optical properties of indium antimonide have been observed in a wide variety of investigations. The role of the photogenerated carrier population in creating optical nonlinearity, however, has not been clearly established. Various theories[1] have been presented which are based on saturation and/or band-edge shifting arguments, but optical measurements to test these hypotheses have been complicated by inexact data regarding nonlinear absorption coefficients and carrier recombination times.

We present results of a novel technique in which the photo-Hall voltage is used to monitor the photocarrier population during nonlinear optical excitation processes. From these observations we present new data, for the characterization of the nonlinear process, which may be important for the optimization of optically bistable devices.

The experimental system consisted of an etalon of InSb (thickness 365 μm, $n \sim 1.16 \times 10^{14}$ cm^{-3}) mounted on a sapphire disk in thermal contact with a cryogenic system to give temperatures of ~77 K. Both the optical transmission and photo-Hall voltage could be measured as a function of the incident power from a cw CO laser. The photo-Hall voltage was obtained with a weak magnetic field ($B \sim 0.01$ T), and the optical measurements were made with a calibrated pyroelectric detection system.

The photogeneration of carriers was investigated as a function of both laser intensity and radiation frequency, and from these results the transition from linear to nonlinear regimes was clearly observed. From measurements in the linear region, the carrier generation characteristic shown in Fig. 1 was obtained. The position of the band edge ($\nu_g \sim 1840$ cm^{-1}) is shown, and the generation curve exhibits a minimum power region for radiation in near resonance with the band gap. The structure of this characteristic may be analyzed from existing linear absorption data[2] to obtain values for the recombination times shown in Fig. 2. This indicates that the recombination time changes from $\tau_R \sim 150$ ns at low absorbing frequencies where bulk recombination dominates to $\tau_R \sim 10$ ns at high absorption where the absorption length is sufficiently small that the carrier generation is within one diffusion length[3] of the surface, and surface recombination is dominant.

In the nonlinear regime, the change in refractive index was sufficient to introduce Fabry-Perot effects. By measuring the photocarrier population change between Fabry-Perot orders a value for the change in refractive index per carrier pair was obtained which can be simply related to the nonlinear refractive index.

Further analysis of the nonlinear region at a fixed frequency and variable intensity yields data for the carrier concentration dependence of the recombination time.

These new results are important for the optimization of InSb optically bistable devices where the performance objectives are lower power operation and minimum switch times. The technique has interesting possibilities for the electrical monitoring of optically bistable states. **(Poster paper)**

1. B. S. Wherrett and N. A. Higgins, Proc. R. Soc. London Ser. A **379,** 67 (1982).
2. D. A. B. Miller, C. T. Seaton, M. E. Prise, and S. D. Smith, Phys. Rev. Lett. **47,** 3 (1981).
3. D. J. Hagan, H. A. MacKenzie, H. A. Al-Attar, and W. J. Firth, Opt. Lett, **10,** 187 (1985).

THGG18 Optical nonlinearities and bistability in a glass–liquid crystal interface

J. A. MARTIN-PEREDA, P. MENENDEZ-VALDES, U. Polytecnica de Madrid, Escuel a Tecnica Superior de Ingenieros de Telecomunicacion, Departamento Electronica Cuantica, 28040 Madrid, Spain.

As reported previously,[1,2] an interface between linear and liquid crystal media shows some nonlinear properties that can be employed in the analysis of this type of optical bistable device.

In trying to achieve a bistable effect similar to the one proposed by Kaplan[3] for a nonlinear Kerr medium, an optimum device would obtain molecular reorientation of an originally homeotropic nematic by interaction with the laser field. We used the experimental setup shown in Fig. 1. The nematic film is a hybrid aligned sandwich of MBBA ($n_e = 1.747$, $n_o = 1.544$) with the homeotropic surface the interface with a F-2 glass prism ($n \simeq 1.63$ for $\lambda = 488$ nm). In these conditions the critical angle was 18.69°. It has been shown[4] that with MBBA, a colored nematic, the main effect responsible for nonlinearities in a glass–homeotropic film interface is a thermal effect due to light absorption. With the hybrid alignment, we expected to reduce the necessary intensity of the evanescent field to get the reorientation that allows frustrated total internal reflection. This goal has been partially reached as can be shown by using samples with different widths. For low intensities, thick samples show linear behavior, while thin ones show nonlinearity and hysteresis [Fig. 2(a)]. From the

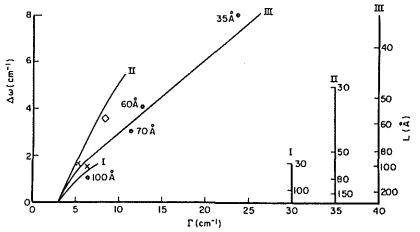

THGG15 Fig. 1. Wave number shift $\Delta\omega$ vs FWHM Γ as a function of size L for spherical Si microcrystals with exponential *I*, sinc *II*, and Gaussian *III* phonon confinement functions. The microcrystal size is indicated when it has been measured independently.

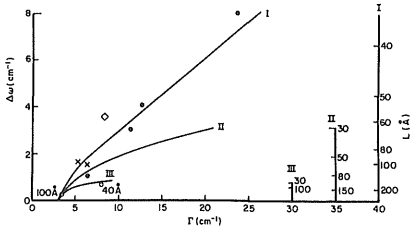

THGG15 Fig. 2. $\Delta\omega$ vs Γ as a function of size L for spherical *I*, cylindrical *II*, and slab *III* Si microcrystals with Gaussian phonon confinement function. Data for spherical and slab microcrystals are also shown.

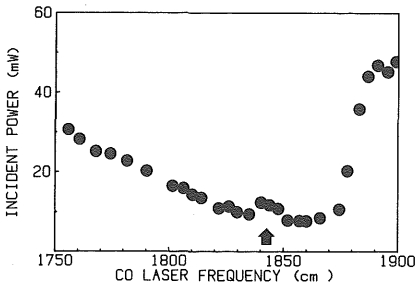

THGG17 Fig. 1. Plot of the incident power to generate 10^{10} carriers as a function of frequency.

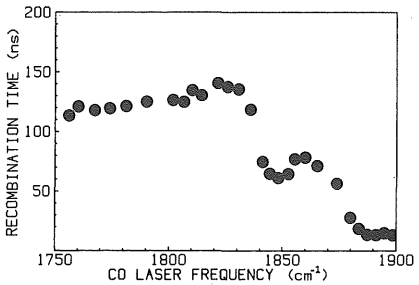

THGG17 Fig. 2. Plot of carrier recombination time vs radiation frequency.

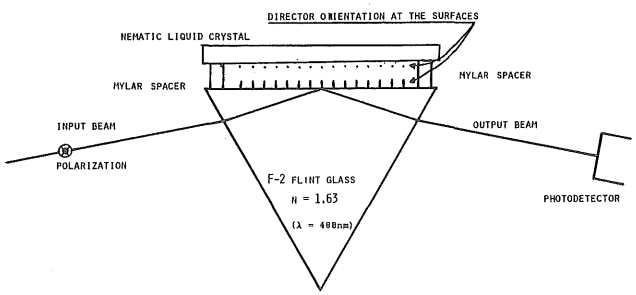

THGG18 Fig. 1. Experimental setup.

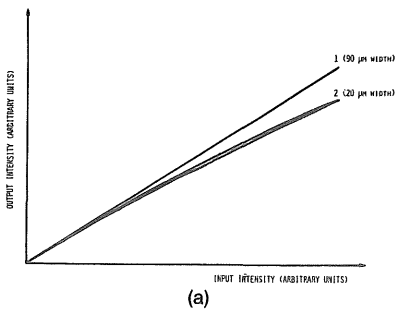

(a)

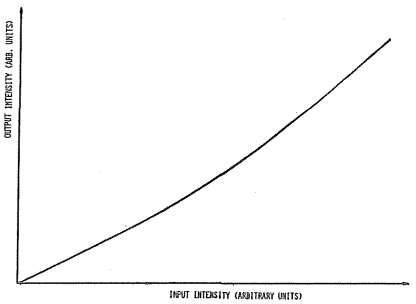

THGG18 Fig. 3. Nonlinear behavior for the MBBA in isotropic phase.

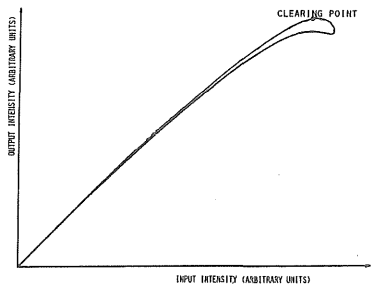

(b)

THGG18 Fig. 2. (a) Behavior for low intensities and several nematic film thicknesses. (b) Hysteresis cycle when the clearing point is reached.

hysteresis cycle and switching conditions, it is possible to show that the thermal effect is still dominant. If the optical field increases in the liquid crystal, heating is easier as films are thinner. By increasing the incident power, the clearing point of MBBA is reached. The whole hysteresis cycle is shown in Fig. 2(b). A bistable behavior is shown, but the low-intensity state depends on the maximum incident intensity, and it is reached after a long time, when the thermal equilibrium is established.

Some other experiments have been carried out with MBBA in isotropic phase to reduce the thermal dependence of the refractive index. In isotropic phase the refractive index of MBBA is ~1.64 with a very smooth variation with temperature. A SF-10 prism ($n \simeq 1.74$ at $\lambda = 514.5$ nm) was employed, and no treatment has been given to the surfaces. The critical angle is now ~19.23°. With total internal reflection, we found no nonlinear behavior with the working intensities (up to 1 kW/mm^2). But if we use an angle greater than the critical one (we have defined angles between the beam and interface), both transmitted and reflected beams show the ring pattern due to reorientation in isotropic phase. Now a clear nonlinearity is observed (Fig. 3). By using a narrow iris and detecting only the central spot, a narrow hysteresis cycle seems to appear, but more accurate experiments should be executed. **(Poster paper)**

1. J. A. Martin-Pereda, in *Technical Digest, Thirteenth International Quantum Electronics Conference* (Optical Society of America, Washington, DC, 1984), paper WII13.
2. J. A. Martin-Pereda, Proc. Soc. Photo-Opt. Instrum. Eng. **492,** 370 (1984).
3. A. E. Kaplan. Sov. Phys. JETP. **45,** 896 (1977).
4. I. C. Khoo, Appl. Phys. Lett. **40,** 645 (1982).

THGG19 Phase conjugation in iron-doped lithium niobate: study and application

YAN-MING LIU, YU LI, JIAN-QUAN YAO, Tianjin U., Department of Precision Instruments, Tianjin, China.

Consider the three transport processes of charge carriers (typically due to $Fe^{2+} \leftrightarrow Fe^{3+}$); with the photovoltaic effect dominating in iron-doped lithium niobate, the photorefractive effects of one-beam incidence and two-wave mixing are analyzed and experiments made. The refractive-index spatial variation diverges the incident beams like a lens in the direction of the *c* axis, which is demonstrated by using a He–Ne laser beam.

Using iron-doped lithium niobate as the nonlinear medium and a He–Ne laser as the light source, the distortion compensation, Doppler-free reflection, and lensless imaging of the phase conjugate waves are demonstrated. We show that only by using symmetrical pump waves can we obtain a phase conjugate wave of high fidelity due to the photorefractive divergence in the crystal. Depending on the direction, polarization, and coherence relationships of the four waves in degenerate four-wave mixing, one grating in the interaction gives rise to strong coupling. The phase conjugate reflectivity is a function of the optical length difference of the two writing beams in the form of $|\sin C|$ in one period. The phase conjugate reflectivity is different for the various angles and polarizations of the incident waves, as observed in the experiments.

We first observed multiple optical phase conjugate waves in forward degenerate four-wave mixing by three waves of the same intensity with the following vectors: $\mathbf{K}_4 = \mathbf{K}_1 + \mathbf{K}_2 - \mathbf{K}_3$ and $\mathbf{K}_4' = \mathbf{K}_2 + \mathbf{K}_3 - \mathbf{K}_1$, $\mathbf{K}_5 = \mathbf{K}_1 + \mathbf{K}_4 - \mathbf{K}_2$ and $\mathbf{K}_5' = \mathbf{K}_3 + \mathbf{K}_4 - \mathbf{K}_2$. These phase conjugate waves are produced by Bragg diffraction of the three incident waves from the gratings they form. Using two probe waves we have also observed two phase conjugate waves with two strong pump waves. We also used multiple probe waves to obtain multiple phase conjugate waves, which is the intrinsic property of the third-order nonlinearity. Analysis shows that there is little decrease in fidelity and reflectivity of the multiple phase conjugate waves compared with those of the one-phase conjugate wave.

Multiple phase conjugation can be used in photolithography, multiphotography, nonlinear spectroscopy, etc. **(Poster paper)**

THGG20 Four-wave mixing in phase conjugation by stimulated Brillouin scattering

QI-HUANG GONG, ZONG-JU XIA, JIA-SUN YANG, Peking U., Physics Department, Beijing, China.

We have prepared several phase plates to observe phase conjugation by stimulated Brillouin scattering in carbon disulfide in the usual way. One of the plates was specially made, lightly ground by fine emery. Its spatial Fourier spectrum shows a very bright spot in the center of the speckle pattern, which means that the light beam that passed through this plate consisted of a strong plane wave component and many weak random components. This is different from the phase plate in phase conjugation by stimulated Brillouin scattering given in earlier papers,[1] but, using only this special plate, we have successfully obtained phase conjugation.

This phase conjugation process cannot be explained well by statistical theory.[2] By comparing the beam structure of the backward scattered light with that of the laser that passed through the special plate and by analyzing the spatial Fourier spectra of the different phase plates used, we give the following explanation. Two nonlinear effects occur in this phase conjugation process: stimulated Brillouin scattering and near degenerate four-wave mixing. The stimulated Brillouin scattering is caused by the strong component of the incident light, and the near degenerate four-wave mixing is formed by the strong component wave, its stimulated Brillouin scattering wave, one of the weak components, and its phase conjugated wave. Considering our experimental conditions, we got a group of equations from the statistical theory that verify our explanation.

Our experiment and its explanation are essentially different from earlier work.[3,4]

(Poster paper)

1. R. A. Fisher, *Optical Phase Conjugation* (Academic, New York, 1983), Chap. 6.
2. V. G. Sidorvich, "Theory of 'Brillouin Mirror'," Zh. Tekh. Fiz. **46,** 2168 (1976) [Sov. Phys. Tech. Phys. **21,** 1270 (1976)].
3. N. G. Basov *et al.*, Kvantovaya Elektron Moscow **6,** 394 (1979) [Sov. J. Quantum Electron. **9,** 237 (1979)].
4. R. L. Abrams, C. R. Giuliano, and J. F. Lam, Opt. Lett. **6,** 131 (1981).

THGG21 Secondary bistable switching at milliwatt powers in nematic phase liquid crystals

A. D. LLOYD, I. JANOSSY, HUGH A. MacKENZIE, Heriot-Watt U., Physics Department, Edinburgh EH14 4AS, U.K.

Thermal switching effects in liquid crystals are of particular interest because of the large value of their temperature coefficient of refractive index ($\partial n/\partial T$). The well-documented purely thermal effect is the primary optical nonlinearity, but we report an additional reorientational effect which can be initiated at milliwatt incident powers from a He–Ne laser to produce a secondary optically bistable switching effect.

For this investigation we constructed resonators from both low-absorption dielectric and high-absorption metallic coatings of glass substrates, with treated surfaces to produce homeotropic alignment of the liquid crystals, and separated by 12-μm spacers to form the resonator dimensions.

Thermal absorption is introduced into the system in two ways, either by the addition of a suitably absorbing dye or from absorption in the reflective coatings which are in thermal contact with the liquid crystal.

With the aluminum-mirrored resonator, we clearly observed the well-documented, thermally switched, bistable characteristic, an example of which, for a specific detuning, is shown in Fig. 1(b). This type of characteristic is analogous to the thermal bistability observed in, say, a ZnSe interference filter,[1] i.e., an irradiance-induced temperature rise tunes the effective optical dimensions of the resonator onto a transmission maxima, hence the dependence on initial detuning. However, compared to ZnSe, the liquid crystal's much higher $\partial n/\partial T$ gives a correspondingly lower switching threshold.

Increasing the incident irradiance past this initial threshold allows us to observe a second switch, detected as an overall reduction in the transmission; this is the down-switch displayed after the first, purely thermal, up-switch in Fig. 1(a) and which gives the second bistable characteristic.

When imaging directly onto the liquid crystal layer, this second switch was observed as the manifestation of a local reorientational effect, which appears as a single, and distinct, dark ring within the liquid crystal layer itself. This effect is also observed, without bistability, in a mirrorless cell.[2]

When observing the characteristics of the dielectric-mirrored, dyed liquid crystal resonators, we find only one bistable switch, this being of the more recognizable (increasing transmission) up-switch type. However, when imaging again on the liquid crystal layer, this switch, although thermally initiated, is characterized by the appearance of the single ring associated previously with the second switch of the all-aluminum cell.

We have demonstrated that these techniques, and the purely thermal effect, can be used to achieve characteristically reproducible bistability at cw milliwatt switching powers and with any wavelength in the visible spectrum.

Current evaluations of the temperature dependence, repolarization, and temporal responses of the reorientational effect will be reported.

(Poster paper)

1. S. D. Smith, J. G. H. Mathew, M. R. Taghizadeh, A. C. Walker, B. S. Wherrett, and A. Hendry, Opt. Commun. **51,** 357 (1984).
2. M. R. Taghizadeh, E. Abraham, and I. Janossy, in *Topical Meeting on Optical Bistability* Dec. 1985 (Springer-Verlag, New York), paper OB3, to be published.

NOVEL PHYSICS WITH LASERS

THGG22 Coherent transients for the study of molecular dynamics in simple liquids

J. D. W. VAN VOORST, D. BRANDT, B. L. VAN HENSBERGEN, U. Amsterdam, Laboratory for Physical Chemistry, 1018 WS Amsterdam, The Netherlands.

The technique of Raman echoes in a vibrational degree of freedom of the nitrogen molecule is described briefly. The essential of this experi-